# Excited State Isomerization Kinetics of 4-(Methanol)Stilbene: Application of the Isodielectric Kramers−Hubbard Analysis

**Kathy L. Wiemers and John F. Kauffman***

*Department of Chemistry, University of Missouri, Columbia, Missouri 65211*

*Received: August 15, 2000*

Trans-4-(methanol)stilbene (HMS) is a member of the diphenylpolyene family with a methanol group appended to one of the phenyl rings of stilbene. In previous studies, we have demonstrated that the polar functional group has a substantial influence on rotational dynamics of HMS in polar liquids and in supercritical $CO_2$. In this paper, we examine the influence of the methanol group on the trans−cis excited state photoisomerization of HMS. We present absorbance and fluorescence spectra that indicate that the spectroscopy of HMS is nearly identical to that of stilbene. We utilize the spectra to calculate the radiative rate constant of the excited-state trans isomer of HMS. Using this result and measured fluorescence lifetimes, we characterize the trans-cis isomerization rate of HMS in a series of *n*-alcohols over temperatures from 0 to 60 °C. Linear Arrhenius plots are observed over this temperature range. We also present an analysis based on the isodielectric Kramers−Hubbard method originally developed by Anderton and Kauffman. The results of this analysis demonstrate that the barrier to trans-cis isomerization of HMS decreases with increasing solvent permittivity.

## 1. Introduction

Trans-to-cis photoisomerization reactions of diphenylpolyenes have been extensively studied over the past two decades as prototypical examples of unimolecular reactions.[1−4] The isomerization reaction of stilbene in solution, in particular, has been studied by many researchers.[5−9] Solvent viscosity is known to play an essential role in determining the rate of these reactions. Analysis of isomerization rates has been performed using the Arrhenius law; however, the activation energies obtained from the calculations do not separate the true barrier energy from the apparent activation energy due to temperature-dependent viscosity. Isoviscosity plots have been used to obtain corrected activation energies.[2,7,10] This method assumes that the viscosity dependence of the isomerization rate appears in the frequency factor and appears to work well for nonpolar, nonassociating solvents, but fails for polar solvents.[2,5,7,8,11,12] Kramers theory is also often used to determine energy barriers, since it includes a functional dependence of the rate constant on solvent friction. The Kramers expression[13] is given by

$$k_{nr} = \frac{\omega_a \xi}{4\pi\omega_b}\left\{\left[1 + \left(\frac{2\omega_b}{\xi}\right)^2\right]^{1/2} - 1\right\}\cdot\exp\left(\frac{-E_a}{kT}\right) \qquad (1)$$

where $\omega_a$ and $\omega_b$ are the initial well frequency and the imaginary barrier frequency, respectively, assuming a piecewise parabolic potential energy surface. $\xi$ is the frictional parameter given in units of frequency. Hydrodynamic theories relate $\xi$ to the solvent viscosity, but hydrodynamics is not appropriate for fast unimolecular isomerizations in which a small reactive body undergoes primarily rotational motion over the course of the reaction. Lee et al.[14] have suggested that $\xi$ be replaced by $\beta$, the angular velocity correlation frequency, when Kramers theory is applied to diphenylpolyene photoisomerization reactions. $\beta$ is given by the Hubbard relation[15]

$$\beta = (6kT/I)\tau_r \qquad (2)$$

where $kT$ is the thermal energy, $I$ is the solute moment of inertia, and $\tau_r$ is the solute rotational correlation time. Lee et al.[14] refer to this as the Kramers−Hubbard model. Note that the Kramers−Hubbard frequency factor can also be derived from Grote−Hynes theory[16] for barrier crossing in solution in which the rate expression is

$$k_{iso} = \frac{\omega_a}{2\pi}\frac{\lambda_r}{\omega_b} \qquad (3)$$

and

$$\lambda_r = \omega_b^2 \int_0^\infty \mathrm{d}t e^{-\lambda_r t}\langle\omega_\phi^2\rangle^{-1}\langle\omega_\phi(0)\omega_\phi(t)\rangle \qquad (4)$$

Here we have replaced the velocity time correlation function in the reactive frequency factor of Grote−Hynes theory with the angular velocity time correlation function, which is appropriate for trans-cis isomerization. $\lambda_r$ can be evaluated in the long time (diffusive) limit by making use of the relation derived by both Steele[17,18] and Hubbard[15]

$$\langle\omega_\phi(0)\omega_\phi(t)\rangle = \frac{kT}{I}e^{-\beta t} \qquad (5)$$

where $\beta$ is given by eq 2. The normalization factor is given by

$$\langle\omega_\phi^2\rangle = \frac{kT}{I} \qquad (6)$$

which yields

$$\lambda_r = \frac{\omega_b^2}{\lambda_r + \beta} \qquad (7)$$

* To whom correspondence should be addressed. E-mail: kauffmanj@missouri.edu.

10.1021/jp002940b CCC: $20.00 
Published on Web 01/17/2001

Solving for $\lambda_r$ and substituting into eq 3 gives the Kramers−Hubbard rate expression.

In recent years, we have undertaken comparative studies of trans-diphenylpolyenes in supercritical fluid solvents with the goal of identifying behavior attributable to fluid clustering in the compressible regime. In the course of these studies, we have found it necessary to examine the diphenylpolyenes in a variety of liquid solvents in order to examine the influence of solvent dielectric properties on the isomerization reaction. Several groups have attempted to analyze these effects,[7,10,19,20] but until recently, no clear relationship between activation barrier and solvent permittivity had been identified. In a previous series of papers,[21−23] we demonstrated a method for the analysis of rate data that allows one to extract the dependence of the isomerization activation energy on the solvent permittivity. We refer to this method as the isodielectric Kramers−Hubbard (IKH) analysis. The method allows us to extract activation energies at constant solvent permittivity by using the Kramers−Hubbard equation to account for solvent viscosity in a series of alcohol-temperature pairs that maintain isodielectric conditions. The method has been applied to stilbene in alcohols and to diphenylbutadiene (DPB) in alcohols and in other polar solvents. In this paper, we have applied the IKH method to *trans*-4-(hydroxymethyl)stilbene (HMS). Though this molecule is expected to be similar to other diphenylpolyenes, it has not been thoroughly investigated. Furthermore, this study extends this method to analysis of a polar solute, which has been shown to experience dielectric friction in hydrogen bonding solvents.[24]

In this paper, we present the results of our recent investigations into the photophysics and isomerization kinetics of HMS in liquid *n*-alcohols. The paper is organized as follows. Experimental methods are described in Section 2. We characterize the spectroscopy of HMS in Section 3, and present some spectroscopic predictions based on semiempirical calculations. We also present a determination of the molecule's radiative lifetime in this section. The results of temperature-dependent fluorescence lifetime studies in a series of *n*-alcohols are presented in Section 4, including analysis by the IKH method. These results identify the dependence of the isomerization barrier height on the solvent permittivity. We discuss these results and their relationship to recent literature on solvent effects in chemical dynamics in Section 5.

## 2. Experimental Section

Trans-4-stilbenemethanol (Aldrich as 98.7%) was used as obtained. Optima grade hexane, 100% ethanol, 1-propanol and 1-butanol were used as obtained. The higher alcohols, 1-pentanol, 1-hexanol, 1-heptanol, and 1-octanol were purchased from ICN Biochemical, Inc. and were fractionally distilled over ground 4 Å molecular sieves. The 1 cm, quartz cuvettes used in these studies were soaked in a Nochromix solution for three minutes, rinsed with deionized water three times, and then rinsed with absolute ethanol to remove trace impurities that can interfere with fluorescence studies of molecules with low quantum yields. Absorbance spectra were obtained using a Hewlett-Packard 8453 diode-array instrument with 1 nm resolution. Fluorescence spectra were measured using a SLM-Aminco 8100 spectrofluorometer. Slit widths were set to 2 nm. All fluorescence spectra were taken with 3 g/L Rhodamine B in propylene glycol as a reference. The excitation wavelength was set to 298 nm, and absorbances were always 0.1 or less. The photomultiplier tubes were offset to null dark current. Fluorescence lifetimes were measured in a series of *n*-alcohols using time-correlated single photon counting.[25,26] A mode-locked Nd:YAG laser was pulse compressed and frequency doubled to provide 5 ps 532 nm pulses at 80 MHz. These pulses synchronously pumped a dye laser with a single birefringence filter. The 0.6 ps pulses from the dye laser were cavity dumped at 4 MHz and frequency doubled in a KDP crystal to generate 300 nm pulses. The fluorescence was collected through a 370 nm band-pass filter and a polarizer set to 54.7° relative to the excitation polarization. The detection electronics have been described elsewhere.[21] Fluorescence lifetimes were extracted by iterative reconvolution using single-exponential model functions. The instrument response function was 53 ps (fwhm), which was determined by measuring the signal from a scattering solution through a 300 nm band-pass filter. The fluorescence lifetimes were measured over a temperature range of 10 to 60 °C. The temperature was controlled to ± 0.1 °C using a Peltier thermoelectric cuvette holder of our own design. Fluorescence anisotropies, *r*, were measured over the same temperature range using a custom-built photon counting fluorometer. Rotational correlation times, $t_r$, were calculated from the steady-state fluorescence anisotropies using the Perrin equation.[25] A complete description of the instrument and a detailed analysis of the rotational diffusion results have been recently published.[24] Briefly, we utilize the steady state method because the rotational diffusion times of HMS in alcohols are fast, having time constants only slightly shorter that the fluorescence lifetimes. This fact hinders the use of time resolved anisotropies because of the difficulty in normalizing the parallel and perpendicular decays. The use of the Perrin equation assumes single exponential anisotropy decays. This assumption is appropriate for diphenylpolyenes, and has been discussed in detail in our recently published study.[24] We use these recent results to calculate $\beta$-values used in the IKH analysis in this paper.

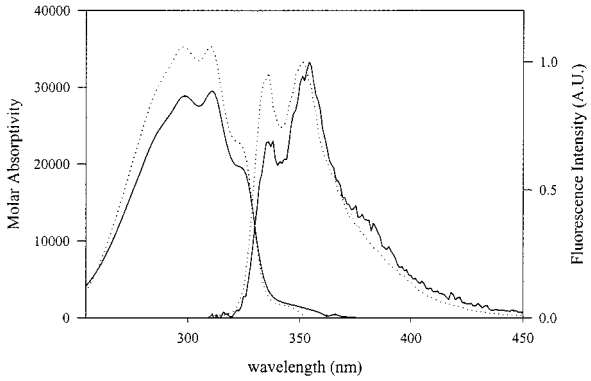


**Figure 1.** Absorbance and fluorescence spectra of HMS in hexane (dotted line) and ethanol (solid line). Absorbance spectra are plotted as molar absorptivity. Fluorescence spectra have been normalized for clarity.

The fluorescence energy, rotational barrier and solvent effects on HMS energy levels were calculated for HMS using semiempirical methods (MOPAC version 93R2). Galvao, et al., showed PM3 to be suitable for stilbene.[27] Spectroscopic evidence suggests that HMS has electronic structure similar to stilbene. Structural optimization (HyperChem) was used to determine moments of inertia for optimized HMS structures, giving the following values: $I_a = 375 \times 10^{-40}$ g/cm$^2$, $I_b = 4940 \times 10^{-40}$ g/cm$^2$, and $I_c = 5306 \times 10^{-40}$ g/cm$^2$.

## 3. Spectroscopy of HMS

Absorbance and fluorescence spectra of trans-HMS in ethanol and hexane are shown in Figure 1. The absorbance spectrum shows peaks at 298 and 310 nm and a shoulder at 324 nm in

**TABLE 1: Relative Peak Absorbances of trans-HMS and trans-Stilbene[a]**

| | HMS | | | Stilbene | | |
|---|---|---|---|---|---|---|
| peak position | 298 | 310 | 324 | 294 | 306 | 320 |
| | relative absorbance | | | | | |
| in hexane | 1 | 1 | 0.64 | 1 | 0.94 | 0.56 |
| in ethanol | 1 | 1.02 | 0.68 | 1 | 0.96 | 0.59 |

[a] The HMS peak separations are identical to those of stilbene. When the spectrum of HMS is shifted 4 nm to the blue it is nearly superimposable onto the stilbene spectrum. Neither compound exhibits a solvatochromic shift between hexane and ethanol, but both compounds exhibit a slight variation in relative peak absorbances between the different solvents.

both solvents. The spectra are nearly identical to one another, differing only in the relative peak absorbances. These are given in Table 1, along with the peak positions and absorbances of trans-stilbene. Beer's Law plots from spectra of known concentration ($1 \times 10^{-5}$ M to $1 \times 10^{-6}$ M range) gave 298 nm molar extinction coefficients of 28 700 ± 2200 L/(mol·cm) in ethanol and 35 400 ± 400 L/(mole·cm) in hexane. We have also observed that the absorption spectrum in ethanol is less stable than the spectrum in hexane in the <250 nm region, a region where the cis isomer of stilbene is known to absorb. This observation is consistent with conclusions that will be drawn in Section 4, indicating that the barrier to excited state photoisomerization is substantially lower in ethanol than in hexane. Thus, a larger fraction of excited HMS molecules relax through the excited-cis conformation when the solute is dissolved in ethanol. The instability of the absorption spectrum also suggests that, following relaxation from the excited cis potential energy well to the ground state, solvent dependent variations in the ground- or excited-state potential energy surfaces may result in a trans−cis branching ratio that favors the ground-state cis isomer in ethanol. Regardless of the cause of this instability, the molar extinction coefficients in ethanol are less reliable that those measured in hexane, and this is made manifest in the large uncertainty of its value.

The fluorescence spectra for HMS in hexane and ethanol are very similar, with peak intensities at 351 and 354 nm, respectively. The small Stokes shift mimics that observed for stilbene and indicates that the emissive species dipole moment is nearly the same as the dipole moment of the ground state species. This result suggests that the methanol group in HMS is not strongly coupled to the aromatic ring. A theoretical value for the fluorescence energy has been calculated using MOPAC with PM3 parametrization. The calculated total energy difference is $1.428 \times 10^{-19}$ cal, which corresponds to 332 nm. Solvent effects on the ground and excited-state energies of HMS were also calculated using a conductor-like screening model (COSMO).[28] The results indicate that ground and excited state energies experience nearly identical shifts as the permittivity of the surrounding medium increases, and are consistent with the small solvatochromic shift observed in the fluorescence spectra.

During our early studies, we observed temporal variations in the fluorescence intensity of HMS. We have also found that after prolonged exposure to strong UV radiation the sample exhibits a decrease of up to 50% in the absorption at 298 nm, particularly for samples dissolved in ethanol. This is accompanied by a slight increase in absorption at about 230 nm where *cis*-stilbene is known to absorb. On the basis of the well-studied trans-cis isomerization of trans-stilbene,[7,29,30] we attribute these observations to the formation of a stable population of cis-HMS in the ground state. It may also be possible that the HMS analogue of dihydrophenanthrene can be formed under strong UV radiation.[29,31] Exposure of HMS to elevated temperature and room light does not result in dramatic changes in the spectra. We have taken great care to ensure that the reported fluorescence spectra and subsequent data analysis are not influenced by these effect through the use of sample stirring, oxygen purging, reduced UV exposure, fast fluorescence scans, and exhaustive repeatability studies.

The radiative rate constant for HMS in hexane and ethanol has been determined by the Strickler−Berg method[32] using the absorbance and fluorescence spectra shown in Figure 1. This method relates the molecule's radiative rate constant to the spectrum of it's molar extinction coefficient and the shape of it's fluorescence spectrum through the expression

$$k_r = 2.880 \times 10^{-9}\, n^2 \langle \nu_f^{-3} \rangle_{av}^{-1} \left(\frac{g_l}{g_u}\right) \int \epsilon \, d(\ln \nu) \qquad (8)$$

where $n$ is the refractive index for the solvent, $\nu$ is the absorbed frequency in wavenumbers, $\langle n_f^{-3} \rangle_{av}^{-1}$ is the reciprocal of the mean cubed inverse frequency of the fluorescence spectrum, $\epsilon$ is the molar extinction coefficient, and $g_l$ and $g_u$ are the degeneracies of the lower and upper states. In the case of HMS, the degeneracy ratio is one. $k_r$ is calculated to be $7.3 \pm 0.8 \times 10^8$ s$^{-1}$ in ethanol and $8.4 \pm 0.8 \times 10^8$ s$^{-1}$ in hexane. The estimated error in the hexane value is 10%, which we determine from our ability to reproduce the same results through repeated experiments. The notably lower value in ethanol may result from anomalously low extinction coefficients due to the unstable nature of trans-HMS in ethanol, and we take this value as a lower limit on the radiative rate constant for HMS. These values are essentially identical with radiative rate constants for other diphenylpolyenes, notably stilbene. Apparently, the methanol substituent does not influence the radiative relaxation rate. For subsequent analysis, we used a value of $k_r$ equal to 8. x $10^8$ s$^{-1}$ in all solvents. Though this choice is somewhat subjective, it reflects the uncertainty in these measurements as well as the increased difficulty of making accurate measurements in ethanol solutions. The radiative rate constant and the fluorescence rate were used to determine the fluorescence quantum yield of HMS. The fluorescence rate was obtained experimentally from fluorescence decays using time-correlated, single-photon counting. These measurements are not expected to be influenced by spectral congestion because the fluorescence quantum yield of *cis*-stilbene is extremely low.[29,31] The room-temperature fluorescence quantum yields for trans-HMS calculated from the Strickler−Berg radiative rate and fluorescence lifetimes are 0.063 (ethanol) and 0.108 (hexane). We have verified these results by relative fluorescence quantum yield measurements from fluorescence spectra using quinine sulfate as a reference standard. The reproducibility of the results was limited by fluorescence intensity variation of HMS, which probably resulted from the depletion of trans-HMS within the interrogation zone. With due attention to the above-mentioned difficulties, we achieve mean values of fluorescence quantum yields that agree within 10% between the Strickler−Berg and integrated fluorescence methods.

With regard to the radiative rate constants, we note that the Strickler−Berg method relies primarily on accurate absorption spectra, which are not influenced by the trans-cis isomerization because the light source is weak and the duration of exposure in the diode array instrument is only a few seconds. Furthermore, with the above-mentioned precautions, the fluorescence spectra were accurate enough to provide reliable measures of the mean

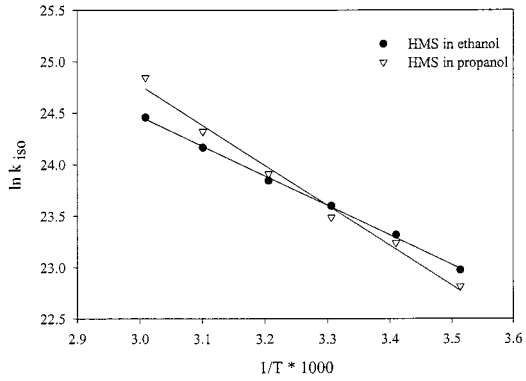


**Figure 2.** Arrhenius plots of HMS in ethanol and propanol. The lines are linear regression fits of the data. Ethanol gave the best correlation coefficient of all the alcohols ($R = 0.998$) and propanol gave the worst correlation coefficient ($R = 0.988$). See Table 2 for additional results.

**TABLE 2: Arrhenius Analysis of Temperature Dependent Rate Constants in Liquids**[a]

| alcohol | slope | $E_a$ (kcal/mol) | intercept | $A$ ($10^{13}$ s$^{-1}$) | $R^2$ |
|---|---|---|---|---|---|
| ethanol | −2870 (2%) | 5.69 (2%) | 33.1 (1%) | 23.43 (22%) | 0.998 |
| propanol | −3900 (5%) | 7.96 (5%) | 36.4 (2%) | 657.08 (100%) | 0.988 |
| butanol | −2970 (2%) | 5.88 (2%) | 33.1 (1%) | 23.43 (22%) | 0.998 |
| pentanol | −3300 (3%) | 6.44 (3%) | 33.9 (1%) | 52.29 (50%) | 0.994 |
| hexanol | −4000 (3%) | 7.84 (3%) | 36.0 (1%) | 437.04 (50%) | 0.995 |
| heptanol | −3900 (3%) | 7.75 (3%) | 35.7 (1%) | 320.91 (50%) | 0.995 |
| octanol | −3600 (6%) | 6.47 (6%) | 34.4 (2%) | 90.16 (80%) | 0.990 |
| hexane | −2610 (3%) | 5.16 (3%) | 31.6 (1%) | 53.18 (35%) | 0.997 |

[a] The linear regression results are used to calculate rate constants for HMS versus temperature and solvent in order to perform the IKH analysis. Uncertainties in the regression results are estimated from standard errors of the fitting parameters, given in parentheses. Activation barriers determined from the slopes do not exhibit a trend with variation in solvent.

inverse cubed fluorescence frequency. On the other hand, the temporal fluctuations in the fluorescence intensity had a profound effect on anisotropy values measured with commercial instrumentation. To overcome this problem, we constructed the modified-T format fluorometer described previously.[24] This instrument is capable of producing accurate anisotropy measurements under the adverse conditions encountered in this study.

### 4. Excited State Trans-Cis Photoisomerization of HMS

The fluorescence lifetimes for HMS in the *n*-alcohol series were measured with the previously described instrument[24] over a range of temperatures. Using the Strickler−Berg radiative rates and the fluorescence lifetimes, trans−cis isomerization rates have been calculated. We obtain the isomerization rate by taking the fluorescence rate and subtracting $k_r$ obtained from the Strickler−Berg formula and the intersystem crossing rate, estimated as $8 \times 10^8$ s$^{-1}$ from literature results for trans-stilbene.[33] The rate constants are then fit to the Arrhenius equation. Figure 2 shows Arrhenius plots of HMS in ethanol and *n*-propanol. These are representative of the plots in all the *n*-alcohols, and are linear over the range of temperatures studied. Ethanol gives the best linear fit of the series, and propanol gives the worst fit. The parameters from the linear least-squares analyses are given in Table 2.

Although Arrhenius plots for diphenylpolyenes are generally linear over limited temperature ranges, the activation barriers obtained from the plots are often in error for two reasons. First, temperature dependent solvent viscosity contributes to the apparent activation barrier, and second temperature dependent solvent permittivity can influence the magnitude of the activation barrier, as discussed below. The viscosity effect has been the subject of extensive investigation.[10,19,20,34] Kramers theory has been widely used to account for viscosity dependence. Keery et al.[34] have demonstrated that in the Smoluchowski regime the temperature dependence of viscosity results in a "preexponential factor" with exponential temperature dependence. Thus the temperature-dependent viscosity contributes an additive term to the Arrhenius activation barrier. In nonpolar solvents isoviscosity plots, in which solvent-temperature pairs are chosen that give constant viscosity, can be used in order to obviate the need to correct for viscosity effects. However, measurements across solvent series such as the current study may suffer from the now-well-known-fact that the relationship between viscosity and rotational diffusion time predicted by the Stokes−Einstein−Debye equation does not hold when the size of the diffusing body approaches the size of the solvent.[22,35,36] Lee et al.[37] have proposed the Kramers−Hubbard method to overcome this difficulty, as discussed in section I. The key advantage of this method is that it offers a means of using experimental observables to characterize the temperature dependence of the preexponential factor in the Kramers expression. Thus, rate constants within a single solvent or across a series of solvents can be properly analyzed with respect to solvent−solute friction.

The second reason to question Arrhenius activation barriers is that they are only correct if the barrier is constant as temperature is varied. This constraint is not met for isomerization of diphenylpolyenes in polar solvents.[11,21] The permittivity of polar solvents such as alcohols can be strongly dependent on temperature, and the transition state for trans-cis isomerization of diphenylpolyenes is polar. Thus, we anticipate temperature-dependent stabilization of the isomerization barrier such that the barrier is diminished as the temperature decreases. We have examined this effect for diphenylbutadiene trans-cis isomerization in alcohols,[11,21] stilbene in alcohols,[23] and diphenylbutadiene in other polar solvents[11] by application of the isodielectric Kramers−Hubbard (IKH) method to the analysis of isomerization rate data. The method relies on Kramers−Hubbard fits of isomerization rate constants and rotational diffusion times for a series of solvent-temperature pairs chosen to maintain a constant solvent permittivity, and the results demonstrate the expected dependence of activation barrier on solvent permittivity. We now apply this method to HMS isomerization rate constants in a series of alcohols.

The IKH method assumes that the Kramers equation characterizes the influence of solute−solvent friction when the Hubbard relation is used, and that only the solvent polarity, characterized by the bulk solvent permittivity, influences the excited-state potential energy surface, on which the isomerization occurs. The method requires rotational diffusion times and isomerization rates across a series of *n*-alcohols at temperatures chosen to maintain a fixed solvent permittivity. These temperature choices are governed by well established relations between temperature and solvent permittivity of the solvent series under investigation.[38] The analysis can be performed across the same series of solvents at different solvent permittivities by adjusting the solvent temperatures. In some cases, the number of solvents that are accessible at a particular solvent permittivity is limited because the required temperature is too near to a phase transition. Once the solvent-temperature pairs for a particular permittivity have been determined, rotational diffusion times and isomerization rates at those temperatures must be found. We have used the experimentally observed linear Arrhenius plots to calculate isomerization rates for HMS at the required temperatures, and

**TABLE 3: Linear Regression Analysis of $\tau_r$ vs $\eta/T$ for HMS in *n*-Alcohols[a]**

| alcohol | slope (ps K/cP) | intercept (ps) | $R^2$ |
|---|---|---|---|
| ethanol | 26 270 | −22.49 | 0.9936 |
| propanol | 25 610 | −54.26 | 0.9793 |
| butanol | 23 900 | −51.49 | 0.9762 |
| pentanol | 15 860 | −6.824 | 0.9918 |
| hexanol | 22 620 | −72.61 | 0.9821 |
| heptanol | 20 020 | −104.65 | 0.9993 |
| octanol | 17 620 | −22.97 | 0.9844 |
| hexane | 36 179 | −10.47 | 0.9734 |

[a] The slopes are used to calculate the rotational correlation time. The RCT values are used in the Hubbard relation to characterize the local solute−solvent friction in the IKH analysis.[39]

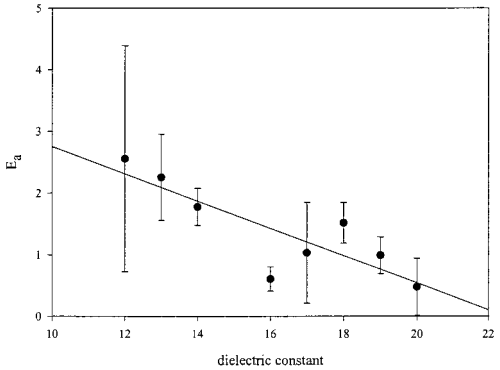


**Figure 3.** Permittivity dependence of the HMS isomerization barrier determined from the IKH analysis of the isomerization rate constants. Each data point is the result of a nonlinear regression fit of at least four solvent-temperature pairs that maintain isodielectric conditions. Temperature, rate constant and $\beta$ are input parameters.

**TABLE 4: Parameters of the IKH Theory for HMS[a]**

| $\epsilon$ | $\omega_a$ ($10^{13}$ s$^{-1}$) | $\omega_b$ ($10^{13}$ s$^{-1}$) | $E_a$ (kcal/mol) |
|---|---|---|---|
| 12 | 1 ± 3 | 4 ± 2 | 2.6 ± 1.8 |
| 13 | 0.8 ± 0.8 | 3.7 ± 0.7 | 2.3 ± 0.7 |
| 14 | 0.4 ± 0.2 | 3.3 ± 0.3 | 1.8 ± 0.3 |
| 16 | 0.2 ± 0.04 | 0.97 ± 0.07 | 0.6 ± 0.2 |
| 17 | 0.2 ± 0.2 | 1.4 ± 0.4 | 1.0 ± 0.8 |
| 18 | 0.4 ± 0.2 | 1.9 ± 0.2 | 1.5 ± 0.3 |
| 19 | 0.17 ± 0.07 | 1.7 ± 0.2 | 1.0 ± 0.3 |
| 20 | 0.08 ± 0.05 | 1.5 ± 0.3 | 0.5 ± 0.5 |

[a] The table shows the isodielectric Kramers−Hubbard fit parameters for HMS. Permittivities 10, 11, and 15 are missing from the table since there were only three points to be fitted within these values.

experimentally observed linear Stokes−Einstein−Debye plots ($\tau_r$ vs $\eta$/T, $\eta$ = solvent viscosity, see Table 3[39]) to calculate rotational diffusion times for HMS at the required temperatures. The latter are found by calculating the temperature-dependent viscosity of a particular solvent-temperature pair, and using the linear regression results of our previous rotational diffusion time study to find $\tau_r$. The Hubbard relation (Equation 2) offers an experimental measure of the local solvent friction in the Kramers analysis by use of rotational diffusion times. $I_c$, the largest inertial moment of HMS ($I_c = 5306 \times 10^{-40}$ g/cm$^2$) has been used to calculate $\beta$. $\beta$, $k_{iso}$ and $T$ serve as data input, and are fit to eq 1 by nonlinear regression with respect to $E_a$, $\omega_a$ and $\omega_b$. $\omega_a$ and $\omega_b$ exhibit a high degree of dependency on one another, which is inevitable given the form of the Kramers expression.

Figure 3 shows a plot of $E_a$ versus solvent permittivity determined from the IKH analysis of HMS over the $\epsilon = 10-20$ range. Parameters determined for each permittivity value are given in Table 4. Each point on the graph represents at least four alcohol-temperature pairs having the specified permittivity. Permittivity values that did not include at least four alcohols within our experimental temperature range were omitted from the plot. Error estimates shown in the plot are the standard errors of the fitting parameters given by the nonlinear regression analysis. Large uncertainties in $\omega_a$ and $\omega_b$, result from fitting a small data set to an equation containing several fitting parameters. Past analysis on DPB[21] showed that increasing the number of data points over a wider temperature range gave smaller uncertainties, but the fit values remained unchanged. The line in Figure 3 is the result of the linear least-squares fit of $E_a$ to the solvent permittivity. The slope of the line is −0.22 kcal/mol (per unit permittivity) with an intercept of 5.0 kcal/mol. The data indicates that the activation energy for HMS ranges from 0.5 to 3.0 kcal/mol in alcohols. The results of the IKH analysis of HMS in alcohols is consistent with the measured value of the activation barrier for HMS in hexane, a solvent with minimal variation in polarity with temperature. Kramers−Hubbard analysis of HMS in hexane gives $E_a = 4.6$ kcal/mol, somewhat lower that the 5.16 kcal/mol Arrhenius parameter. (The difference in these results reflects the viscosity activation energy.) Comparison of the hexane Kramers−Hubbard barrier with the linear regression result in Figure 3 demonstrates excellent agreement between the predicted permittivity dependence of the barrier height based on measurements in polar liquids and the measured barrier height of HMS isomerization in a nonpolar liquid.

## 5. Discussion

We have drawn two primary conclusions from this work. First, it is apparent that HMS is spectroscopically similar to stilbene. Note that the absorption and emission spectra of HMS are no more sensitive to solvent polarity than stilbene, and that both of these solutes have similar radiative rate constants. These observations can be qualitatively explained by the absence of conjugation between the stilbene chromophore and the polar portion of the methanol moiety. Second, we have concluded that excited state trans−cis photoisomerization of HMS, like stilbene and DPB, proceeds over a barrier whose height increases linearly with decreasing solvent permittivity.[21−23]

In hexane, the HMS barrier (4.6 kcal/mol) is somewhat larger than stilbenes (∼4 kcal/mol), an observation that is consistent with barriers of other para-substituted stilbenes. This may simply reflect the increase in the inertial moment along the reaction coordinate in solvents where solvent friction plays a dominant role in governing kinetics. Previous analysis of stilbene in alcohols has suggested that its barrier is less than 1 kcal/mol.[1,34] However, those analyses overlooked the dependence of the solvent permittivity (and therefore the barrier) on temperature. The IKH method attempts to address this issue. When applied to stilbene the IKH analysis reveals a barrier that varies from about 1 kcal/mol at $\epsilon = 20$ to a barrier of about 3.7 kcal/mol at $\epsilon = 10$. The IKH analysis of HMS in alcohols reveals a similar trend, but the barrier is somewhat lower across the entire range of permittivities. Apparently, the methanol substituent of HMS reduces the excited-state barrier to isomerization. The methanol group is also known to influence the overall rotational dynamics of the solute, as shown in our previous study.[24] This should have the effect of reducing the rate of the isomerization reaction. On the other hand, the relatively low barrier to trans-cis isomerization of HMS compensates for the additional viscous drag experienced by the isomerizing fragments. Thus the measured isomerization rates of stilbene and HMS are very similar to one another.

One important question that still remains is how the methanol substituent lowers the barrier of HMS relative to that of stilbene.

It may influence the potential energy surface directly through a symmetry breaking interaction, for example. However, a comparison of HMS and stilbene kinetics in hexane provides evidence that contradicts this suggestion. On the other hand, the presence of the polar functional group results in strong solvent−solute interactions that may encourage an external influence on the potential energy surface. Kurnikova et al.[40,41] have demonstrated that attractive solvent−solute interactions mediate solute motion (and therefore, unimolecular isomerization) by a complex mechanism that includes the expected attractive contribution usually assigned to dielectric friction and the expected repulsive contribution from mechanical friction (i.e., collisions), but also includes an additional contribution from repulsive interactions that result from a large local density attributable to the same attractive solvent−solute interactions. We have interpreted solvent-dependent barriers in stilbene and diphenylbutadiene revealed in our previous studies as resulting from the stabilizing influence of the polar solvent on the transition state to isomerization. Within the framework of that interpretation, the presence of the methanol group on HMS appears to result in a stronger dependence of the isomerization barrier on solvent permittivity. Generalizing the results of Kurnikova et al.,[40,41] the diminished barrier of HMS in alcohols may result from an effective increase in the density of polar molecules around the solute due to an "electrostrictive" influence of the methanol moiety.

Solvent−solute interactions between HMS and alcohols may also alter the potential energy surface of the excited state reaction. The fact that the absorbance of an ethanol solution appears to be more sensitive to exposure to strong UV radiation than a hexane solution suggests that the ground state cis isomer is more easily formed following photoexcitation in ethanol than in hexane. This may reflect a shift in the position of the excited cis potential energy well with respect to the ground-state potential energy surface, resulting in a solvent dependent variation in the ground-state trans-cis branching ratio.

**Acknowledgment.** This research was supported by the National Science Foundation (Grant No. CHE-9508744).

## References and Notes

(1) Waldeck, D. H. *Chem. Rev.* **1991**, *91*, 415.
(2) Velsko, S. P.; Fleming, G. R. *J. Chem. Phys.* **1982**, *76*, 7335.
(3) Andrews, J. R.; Hudson, B. S. *J. Chem. Phys.* **1978**, *68*, 4587.
(4) Brey, L. A.; Schuster, G. B.; Drickamer, H. G. *J. Chem. Phys.* **1979**, *71*, 2765.
(5) Sundstrom, V.; Gillbro, T. *Ber. Bunsen-Ges. Phys. Chem.* **1985**, *89*, 222.
(6) Kim, S. K.; Fleming, G. R. *J. Phys. Chem.* **1988**, *92*, 2168−2172.
(7) Kim, S. K.; Courtney, S. H.; Fleming, G. R. *Chem. Phys. Lett.* **1989**, *159*, 543−548.
(8) Sundstrom, V.; Gillbro, T. *Chem. Phys. Lett.* **1984**, *109*, 538.
(9) Akesson, E.; Bergstrom, H.; Sundstrom, V.; Gillbro, T. *Chem. Phys. Lett.* **1986**, *126*, 385.
(10) Hicks, J. M.; Vandersall, M. T.; Sitzmann, E. V.; Eisenthal, K. B. *Chem. Phys. Lett.* **1987**, *135*, 413.
(11) Anderton, R. M.; Kauffman, J. F. *J. Phys. Chem.* **1995**, *99*, 14 628−14 631.
(12) Courtney, S. H.; Fleming, G. R. *J. Chem. Phys.* **1985**, *83*, 215.
(13) Kramers, H. A. *Physica* **1940**, *7*, 284.
(14) Lee, M.; Bain, A. J.; McCarthy, P. J.; Han, C. H.; Haseltine, J. N.; Smith, A. B., III.; Hochstrasser, R. M. *J. Chem. Phys.* **1986**, *85*, 4341.
(15) Hubbard, P. S. *Phys. Rev.* **1963**, *131*, 1155.
(16) Grote, R. F.; Hynes, J. T. *J. Chem. Phys.* **1980**, *73*, 2715.
(17) Steele, W. A. *J. Chem. Phys.* **1963**, *38*, 2404−2410.
(18) Steele, W. A. *J. Chem. Phys.* **1963**, *38*, 2411−2418.
(19) Sivakumar, N.; Hoburg, E. A.; Waldeck, D. H. *J. Chem. Phys.* **1989**, *90*, 2305.
(20) Zeglinski, D. M.; Waldeck, D. H. *J. Phys. Chem.* **1988**, *92*, 692.
(21) Anderton, R. M.; Kauffman, J. F. *J. Phys. Chem.* **1994**, *98*, 12 125−12 132.
(22) Anderton, R. M.; Kauffman, J. F. *J. Phys. Chem.* **1994**, *98*, 12 117−12 124.
(23) Anderton, R. M.; Kauffman, J. F. *Chem. Phys. Lett.* **1995**, *237*, 145−151.
(24) Wiemers, K. L.; Kauffman, J. F. *J. Phys. Chem.* **2000**, *104A*, 451−457.
(25) Lakowicz, J. R. *Principles of Fluorescence Spectroscopy*; Plenum Press: New York, 1983.
(26) O'Connor, D. V.; Phillips, D. *Time-Correlated Single Photon Counting*; Academic Press: New York, 1983.
(27) Galvao, D. S.; Soos, Z. G.; Ramasesha, S.; Etemad, S. *J. Chem. Phys.* **1993**, *98*, 3016−3021.
(28) Klamt, A.; Schuurman, G. *J. Chem. Soc., Perkin Trans. 2* **1993**, *5*, 799−805.
(29) Repinec, S. T.; Sension, R. J.; Szarka, A. Z.; Hochstrasser, R. M. *J. Phys. Chem.* **1991**, *95*, 10 380−10 385.
(30) Todd, D. C.; Fleming, G. R.; Jean, J. M. *J. Chem. Phys.* **1992**, *97*, 8915−8925.
(31) Petek, H.; Yoshihara, K.; Fujiwara, Y.; Lin, Z.; Penn, J. H.; Frederick, J. H. *J. Phys. Chem.* **1990**, *94*, 7539−7543.
(32) Strickler, S. J.; Berg, R. A. *J. Chem. Phys.* **1962**, *37*, 814.
(33) Brey, L. A.; Schuster, G. B.; Drickamer, H. G. *J. Am. Chem. Soc.* **1979**, *101*, 129.
(34) Keery, K. M.; Fleming, G. R. *Chem. Phys. Lett.* **1982**, *93*, 322.
(35) Dote, J. L.; Kivelson, D.; Schwartz, R. N. *J. Phys. Chem.* **1981**, *85*, 2169.
(36) Gierer, A.; Wirtz, K. *Z. Naturforsch.* **1953**, *8*, 532.
(37) Lee, M.; Holtom, G. R.; Hochstrasser, R. M. *Chem. Phys. Lett.* **1985**, *118*, 359.
(38) Maryott, A. A.; Smith, E. R. *Table of Dielectric Constants of Pure Liquids, NBS Circular 514*; U.S. Government Printing Office: Washington D. C., 1951.
(39) During the course of the present analysis, we identified some minor errors in Table 3 of ref 24, which gave a set of boundary condition factors derived from slopes of Stokes−Einstein−Debye plots. For the most part, these errors were less than 10% of the published values, but for pentanol and octanol, the reported boundary conditions are in error by about 15%. Slopes in Table 3 of the present paper report correct slopes. These errors do not affect the conclusions of ref 24. An erratum will be submitted to correct ref 24.
(40) Kurnikova, M. G.; Balabai, N.; Waldeck, D. H.; Coalson, R. D. *J. Am. Chem. Soc.* **1998**, *120*, 6121−6130.
(41) Kurnikova, M. G.; Waldeck, D. H.; Coalson, R. D. *J. Chem. Phys.* **1996**, *105*, 628−638.